





LETTER

Synchronous effects produce cycles in deer populations and deer-vehicle collisions

Thomas L. Anderson,^{1,2*} 
 Lawrence W. Sheppard,² 
 Jonathan A. Walter,^{2,3} 
 Robert E. Rolley⁴ and
 Daniel C. Reuman^{2,5*} 

Abstract

Population cycles are fundamentally linked with spatial synchrony, the prevailing paradigm being that populations with cyclic dynamics are easily synchronised. That is, population cycles help give rise to spatial synchrony. Here we demonstrate this process can work in reverse, with synchrony causing population cycles. We show that timescale-specific environmental effects, by synchronising local population dynamics on certain timescales only, cause major population cycles over large areas in white-tailed deer. An important aspect of the new mechanism is specificity of synchronising effects to certain timescales, which causes local dynamics to sum across space to a substantial cycle on those timescales. We also demonstrate, to our knowledge for the first time, that synchrony can be transmitted not only from environmental drivers to populations (deer), but also from there to human systems (deer-vehicle collisions). Because synchrony of drivers may be altered by climate change, changes to population cycles may arise via our mechanism.

Keywords

Moran effect, population cycle, population dynamics, synchrony, white-tailed deer.

Ecology Letters (2020)

INTRODUCTION

Population cycles have intrigued ecologists for over 100 years (Myers, 2018). An early hypothesis for the cause of cycles, for the Canadian lynx-snowshoe hare system and other systems, posited that strongly cyclic environmental phenomena such as sun spots may drive population cycles (Sinclair *et al.*, 1992; Selas *et al.*, 2004). The sun spot hypothesis was refuted, however (Nilssen *et al.*, 2007; Myers and Cory, 2013), and whereas it is now recognised that environmental drivers can alter cycles through their interactions with intrinsic population processes (Watson *et al.*, 2000; Kausrud *et al.*, 2008), for decades research has focused instead on explanations of the origin of cycles which involve nonlinear or delayed density dependence, often via predator-prey interactions and parasitism (Kausrud *et al.*, 2008; Krebs, 2013; Myers and Cory, 2013; Martínez-Padilla *et al.*, 2014; Krebs *et al.*, 2018).

Population cycles are fundamentally linked with spatial synchrony, the tendency for geographically distinct populations to exhibit correlated temporal fluctuations. Theory predicts that cyclic populations can be synchronised via weak coupling from dispersal or via shared exogenous forcing (Moran effects), in a process known as nonlinear phase locking (Bjørnstad, 2000). Empirical evidence from laboratory experiments (Vasseur and Fox, 2009; Hopson and Fox, 2019) and observational data (Haynes *et al.*, 2019) support these predictions. Indeed, the lynx-hare system features cycles thought to

be synchronised regionally by phase locking through Moran effects (Stenseth *et al.*, 1999, 2004). As a consequence, the prevailing paradigm is that cycles and synchrony are linked because populations whose dynamics are intrinsically cyclic are easy to synchronise: population cycles help cause spatial synchrony.

We here propose a mechanism by which the direction of causality can be reversed: instead, spatial synchrony can give rise to population cycles. The mechanism comprises the following two steps. First, an exogenous driver synchronises non-cyclic local population fluctuations *on a particular timescale*. Many large climate phenomena fluctuate, episodically or consistently, with emphasis on particular timescales. For example, from ca. 1965–1995, the North Atlantic Oscillation (NAO) contained a substantial 10-year oscillatory component (Sheppard *et al.*, 2016). Thus local weather variables influenced by climatic oscillations can contain periodic components which are synchronous across large areas. These components may be weak and therefore hardly noticeable, in comparison with asynchronous, local fluctuations with which they are combined. Synchronous periodic components in local weather can nevertheless propagate, via Moran effects, to produce weak, synchronous periodic components in local population dynamics. Timescale-specific spatial synchrony of populations is probably common (Defriez *et al.*, 2016; Sheppard *et al.*, 2016, 2017, 2019; Defriez and Reuman, 2017a,b; Walter *et al.*, 2017; Anderson *et al.*, 2019; Haynes *et al.*,

¹Department of Biology, Appalachian State University, 572 Rivers St., Boone, NC 28608, USA

²Department of Ecology and Evolutionary Biology and Kansas Biological Survey, University of Kansas, 2101 Constant Ave, Lawrence, KS 66049, USA

³Department of Environmental Sciences, University of Virginia, 291 McCormick Rd, Charlottesville, VA 22904, USA

⁴Wisconsin Department of Natural Resources, 101 S. Webster St., Madison, WI 53707, USA

⁵Laboratory of Populations, Rockefeller University, 1230 York Ave., New York, NY 10065, USA

TLA current address:

Department of Biology, Southern Illinois University Edwardsville, Box 1651, Edwardsville, IL 62025, USA

*Correspondence: E-mail: anderstl@gmail.com (or) reuman@ku.edu

2019). Second, the weak periodic components of local population dynamics, being synchronous across space, reinforce each other in the total regional population, whereas stronger, asynchronous components on other timescales cancel in the spatial total. Thus periodicities in dynamics which may be unnoticeable at the local spatial scale become dominant at the regional scale. The key here is that synchrony occurs on a *particular timescale*. Dynamics of the total, regional population are then dominated by a cycle on that timescale. See Fig. 1 for a simulated example. A theoretical approach is summarised below and elaborated in Supporting Information (SI) section S1. The bulk of the paper presents empirical evidence for the mechanism.

One potential applied concern is that if fluctuations in local time series do become amplified in a timescale-specific manner as outlined above, outbreaks of pests or disease could follow (Rohani *et al.*, 1999). For example, timescale-specific synchrony of local populations of pests may produce cycles in the regional total pest population and therefore in the damage they cause. Timescale-specific synchrony could also be important for industries, such as hunting, that exploit multiple populations across space if it causes cycling in the regional total population. If the time series of Fig. 1d–f were deer populations in counties within a state so that Fig. 1j–l are state-total populations, differences between the scenarios of Fig. 1 could impact the hunting industry. Cycles may then also cause cascading effects on human economic and social systems.

The ecological system for which we explore the importance of these idea centres on white-tailed deer (*Odocoileus virginianus*) populations across the state of Wisconsin (WI), USA, and on rates of deer-vehicle collisions (DVCs). White-tailed deer is a species of interest due to its economic and cultural benefits and ecosystem impacts (Côté *et al.* 2004; Conover, 2011). Across the USA in 2011, US\$34Bn were spent hunting big game, including deer (U.S. Department of the Interior *et al.* 2011). In WI, hunting-related economic activity is about 1% of state GDP (U.S. Department of the Interior *et al.* 2011). DVCs cause about 50 human fatalities and US\$1.5Bn in vehicular damage annually across the USA (Conover, 2011). Thus it is an important question what drives the year-to-year variability in statewide deer abundance and DVC totals. We consider potential drivers of deer populations including both environmental factors and the direct effects of hunting. We use data from 1981 to 2016 (Fig. 2) aggregated at three spatial resolutions: counties ($N=71$), United States Department of Agricultural (USDA) districts ($N=9$), and statewide (*Methods*).

Here we demonstrate, using theory and deer data, how timescale-specific spatial synchrony can produce regional population cycles. We also show that timescale-specific deer population synchrony begets timescale-specific synchrony in DVCs across the state, producing cycles in state-total DVCs as well. Fluctuations in deer population abundances in the counties of Wisconsin were synchronous due to fluctuations in winter climate, and synchrony occurred mainly on 3- to 7-year timescales. Deer synchrony in turn produced synchrony in DVCs on 3- to 7-year timescales. Timescale-specific synchrony caused substantial fluctuations on 3- to 7-year timescales in both state-total deer populations and DVCs. Our results provide a theoretical description and empirical

support for a new mechanism of cycles, and for its potential applied importance. In contrast to the well-understood mechanism by which cycles can beget synchrony, our mechanism shows that synchrony, when specific to certain timescales, can also produce cycles.

SUMMARY OF THEORY

The statement of our main theoretical result requires a conceptual understanding of the *power spectrum* (or, simply, *spectrum*) of a population or other time series, and of the *cospectrum* of two time series. The spectrum is useful for studying population cycling because peaks in the spectrum indicate cyclic dynamics. Given a time series or stochastic process, $w_i(t)$, measured in location i , the spectrum $S_{w_i w_i}(f)$ is a function of frequency, f . The frequency of a periodic oscillation is one over its timescale, that is, one over its period. The value of the spectrum $S_{w_i w_i}(f)$ is larger for frequencies on which $w_i(t)$ oscillates with greater strength. So, for instance, a population that exhibits strong (respectively, weak) 10-year timescale oscillations will have a spectrum with a large (respectively, small) peak at the frequency $1/10\text{yr}^{-1}$. The spectrum decomposes the variance, $\text{var}(w_i(t))$, according to the timescales on which it occurs, that is, an appropriate integral of $S_{w_i w_i}(f)$ across all frequencies equals $\text{var}(w_i(t))$. The cospectrum of two time series, $w_i(t)$ and $w_j(t)$, decomposes their covariance, $\text{cov}(w_i(t), w_j(t))$, in a similar way: the cospectrum, $C_{w_i w_j}(f)$, is a function of frequency with peaks occurring at frequencies for which oscillations in $w_i(t)$ and $w_j(t)$ are strong and coincident in their phases, that is, synchronous; an integral of $C_{w_i w_j}(f)$ equals $\text{cov}(w_i(t), w_j(t))$.

Our main theoretical result expresses the spectrum, S_{tot} , of a total population across a region composed of $i=1, \dots, N$ local areas in the form

$$S_{\text{tot}}(f) = F_{\text{popdyn}}(f) \left[\sum_{i=1}^N S_{\varepsilon_i \varepsilon_i}(f) + \sum_{\substack{i,j=1 \\ i \neq j}}^N C_{\varepsilon_i \varepsilon_j}(f) \right], \quad (1)$$

where $F_{\text{popdyn}}(f)$ reflects population dynamics within the local areas, and the $S_{\varepsilon_i \varepsilon_i}$ are spectra and the $C_{\varepsilon_i \varepsilon_j}$ are cospectra of environmental noise time series in the local areas. This result is for a model exhibiting autoregressive moving average (ARMA) dynamics within a habitat patch, and $F_{\text{popdyn}}(f)$ is a function that depends only on the ARMA coefficients (Supporting Information section S1). If dynamics are not intrinsically cycling, then $F_{\text{popdyn}}(f)$ has no peaks and does not contribute to whether S_{tot} is peaked. The term $\sum_{i=1}^N S_{\varepsilon_i \varepsilon_i}(f)$ in (1) encapsulates the effects of periodicities in local environmental noise time series on whether the total population exhibits cycling. The term $\sum_{i \neq j} C_{\varepsilon_i \varepsilon_j}(f)$ in (1) encapsulates the effects

of timescale-specific synchrony on whether the total population exhibits cycling. The key observation here is that, when N is large so that the region being considered is a combination of a large number of local areas, the first term is likely to make a smaller contribution to S_{tot} than the second term; the first term is a sum of only N quantities and the second is a sum of $N^2 - N$ quantities, and $N^2 - N \gg N$ for large N . Thus

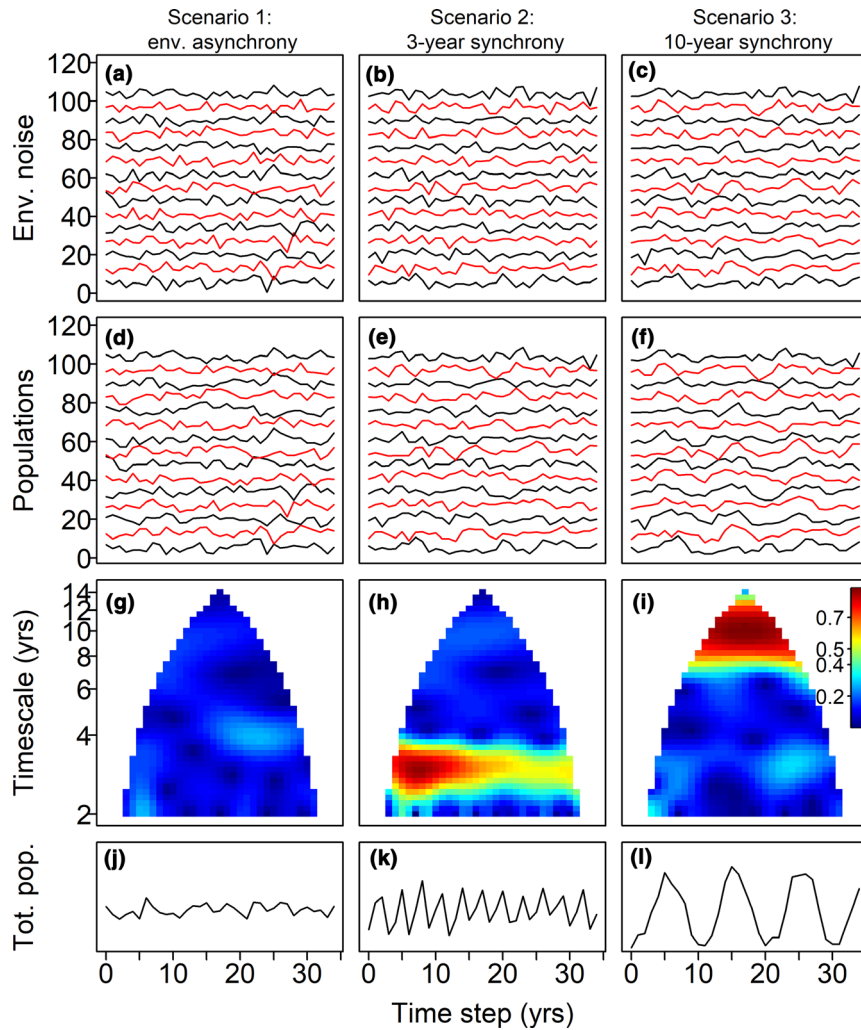


Figure 1 Simulations demonstrating our mechanism whereby timescale-specific synchrony can cause population cycling. Three scenarios with different patterns of environmental synchrony result in different outcomes: scenario 1, an asynchronous-environment scenario, results in no population synchrony or cycling; scenario 2 has environmental synchrony on a 3-year timescale, resulting in 3-year population synchrony and 3-year regional-scale cycles; scenario 3 has environmental synchrony on a 10-year timescale, resulting in 10-year population synchrony and 10-year cycles. In scenario 1, environmental noise in location i ($i = 1, \dots, 71$; first 15 locations shown in (a)) was modelled as $e_i^{(1)}(t) = \sin(2\pi t/w^{(1)} + 2\pi u_i^{(1)}) + 3e_i^{(1)}(t)$, where $w^{(1)} = 3$, the $u_i^{(1)}$ were independent draws from the uniform distribution on $(0, 1)$, and the local noises $e_i^{(1)}(t)$ were standard normal and independent across locations and times. In scenario 2, noise (15 locations shown in (b)) was $e_i^{(2)}(t) = \sin(2\pi t/w^{(2)} + 2\pi u^{(2)}) + 3e_i^{(2)}(t)$ where $w^{(2)} = 3$, $u^{(2)}$ was one single standard normally distributed random number used for all locations, and the $e_i^{(2)}(t)$ were again standard normal and independent. Noise for scenario 3 (c), was like scenario 2 but used $w^{(3)} = 10$. Thus the noises in scenarios 2 and 3 had weak and not visually obvious timescale-specific synchrony and those in 1 had no synchrony. Populations were modelled as $p_i^{(s)}(t+1) = \rho p_i^{(s)}(t) + e_i^{(s)}(t)$ using $\rho = 0.4$ for scenarios $s = 1, 2, 3$, and are displayed (d–f) for locations 1–15. Although population synchrony was weak and cannot readily be detected visually, wavelet mean field magnitude plots (*Methods*) revealed that synchrony was present, in scenarios 2 and 3, on 3- and 10-year timescales (g–i); on such plots, higher values mean greater synchrony at the given time on the given timescale. Total populations (j–l) show clear cycling in scenarios 2 and 3, of periods 3 and 10, respectively, consistent with the proposed mechanism from the *Introduction*: synchrony on a given timescale produces cycling on that timescale in the total population. We used 71 locations because the empirical analyses of this study focus on white-tailed deer populations in Wisconsin, and Wisconsin has 71 counties for which deer data were available. Time series on (a–f) were shifted vertically for readability.

theory predicts that timescale-specific patterns of synchrony are very important for whether spatial-total populations exhibit cycling. Of course, which of the two terms in brackets in (1) is larger depends not only on the number of summands in each term, but also on their values. We explore reasonable scenarios in the Supporting Information and find that the initial intuition is correct, that timescale-specific synchrony is often a very important determinant of regional population cycles. See Supporting Information section S1 for the theory and for examples, including Figs S1, S2 and S3.

METHODS

Empirical data

Using data provided by the Wisconsin Department of Natural Resources (WIDNR), we calculated annual deer abundance estimates for the period 1981–2016 for each of 71 WI counties; and an index of hunter abundance for each county for 1992–2016. We obtained estimates of DVCs for each county for 1987–2016 from the WI Department of Transportation

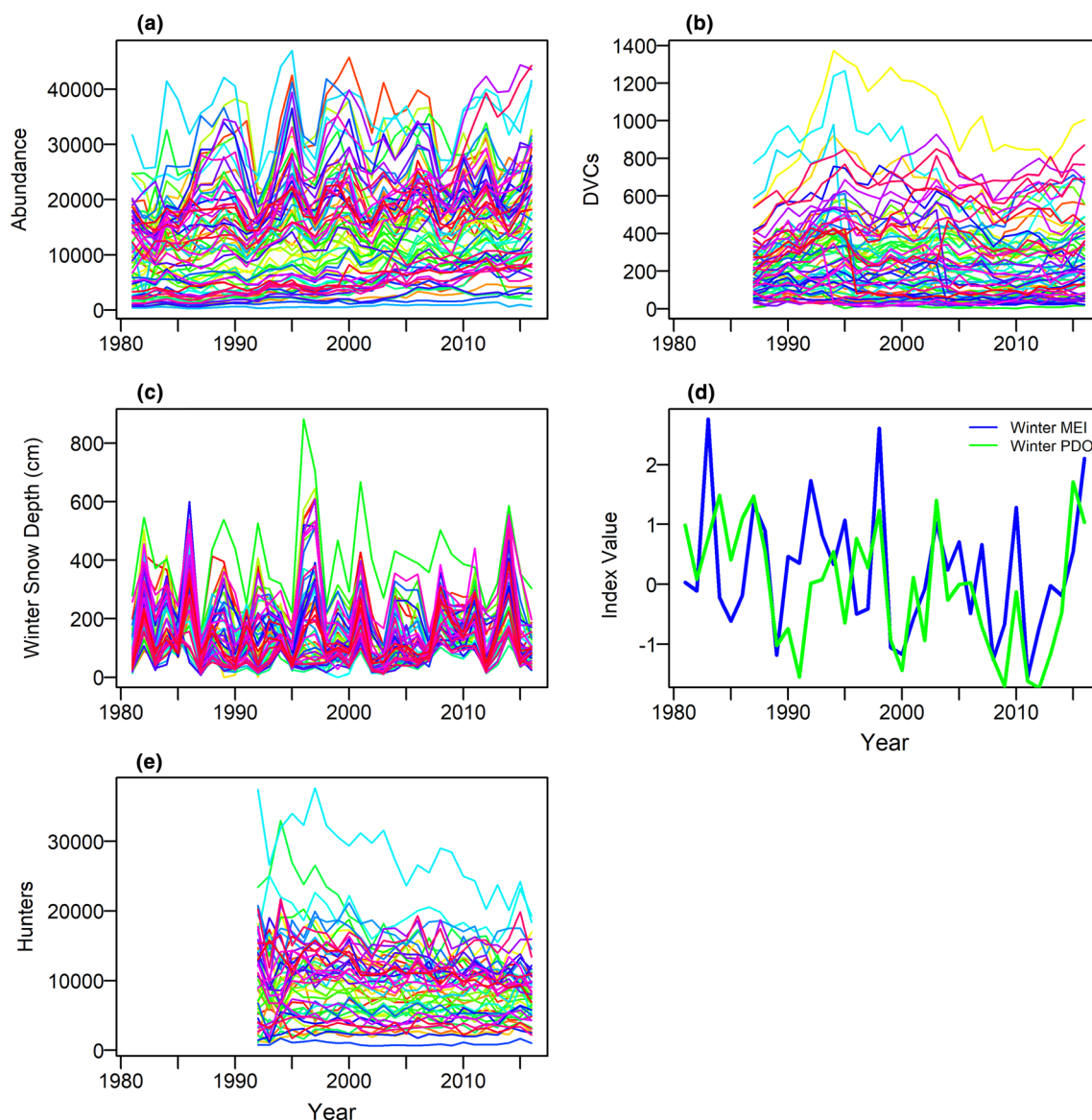


Figure 2 Raw time series of (a) deer abundance, (b) deer-vehicle collisions (DVCs), (c) average winter (Dec_{t-1} to Mar_t) snow depth, and (d) winter climate indices (Multivariate El Niño Southern Oscillation Index, MEI; Pacific Decadal Oscillation, PDO) and hunter abundances (e). Each line in (a–c), (e) represents a county. Other variables were used in analyses (see text) but are not shown here due to lack of significant associations with the deer and DVC variables that were the focus of the study.

(WIDOT), as well as traffic volume estimates (millions of miles driven per county) for 1988–2016, to control for traffic in our analysis of DVCs. We obtained daily weather station data from the National Climatic Data Center (<https://www.ncdc.noaa.gov/>) and performed averaging to produce annual time series of winter (Dec_{t-1} to Mar_t) weather by county for snow depth, precipitation amount and minimum and maximum air temperature – here called Tmin and Tmax. We also calculated a Winter Severity Index (WSI), previously known to relate to winter impacts on deer populations (WIDNR 2001). Winter and growing-season (Apr–Nov) annual time series for the NAO, the multivariate El Niño Southern Oscillation Index (MEI) and the Pacific Decadal Oscillation (PDO) were obtained by averaging monthly values. All of these have been shown to influence large ungulate population dynamics

in North America (Post and Stenseth, 1998; Post and Forchhammer, 2004; Ciuti *et al.*, 2015). High values of these indices generally correspond to mild winter weather over WI (Rodionov and Assel, 2003). Thus a total of 11 weather and climate variables were used: winter Tmin, Tmax, snow depth, and precipitation; winter NAO, MEI, and PDO; growing-season NAO, MEI and PDO; and the WSI. See Fig. 2 for plots of some data, and Supporting Information section S2 for details of all data and methods.

Data pre-processing

We performed all analyses described below at the three spatial scales mentioned in the *Introduction*: counties ($N=44-71$, depending on the variables involved, see Supporting

Information section S2; mean county area \pm SD = 2017 \pm 805 km²), USDA districts ($N=9$; mean district area \pm SD = 16139 \pm 6168 km²) and statewide (Fig. S4). USDA district data were the sum or average of county-level variables, as districts were always conglomerates of counties (Fig. S4); likewise for statewide data. Results remained unchanged in their main substance using larger spatial scales (see *Results*).

Each time series was Box–Cox transformed to ensure Gaussian marginal distributions (Sheppard *et al.*, 2016), which are necessary for the Fourier-surrogate-based spatial wavelet coherence testing procedures described below. This process also included linear detrending, to remove trends that might otherwise obscure patterns of synchrony (Buonaccorsi *et al.*, 2001), as well as variance standardisation (Supporting Information section S2).

Analysis

We use wavelet transforms in all analyses. Wavelets are ideal for detecting periodic components in complex field data (Addison, 2002). The methods we use are well established, standard tools in many fields, or are simple extensions thereof. So we provide in the main text an operational description, only, of each method, that is, what it takes as input, what it provides as output and how to interpret the output, with technical details in Supporting Information section S2. All wavelet analyses were done via the open-source “wsyn” software package for the R language (Reuman *et al.*, 2019).

We characterised the spatial synchrony of spatiotemporal variables (e.g. deer abundance) using wavelet mean field magnitudes and wavelet phasor mean field magnitudes. Both methods take as input standardised (see above) time series data from multiple locations and provide as output plots which display the degree of synchrony among locations as a function of time and timescale (Figs 1g–i, Fig. S5). Thus the plots reveal at what times, during the duration of data collection, and on what timescales, synchrony was prevalent. The wavelet phasor mean field magnitude plot describes the degree of phase synchrony among time series, whereas the wavelet mean field magnitude plot describes the degree of synchrony in both phases and amplitudes of oscillation. The statistical significance of a wavelet phasor mean field magnitude plot, at any given time and timescale, can be assessed through comparison to a null hypothesis of random phases (Supporting Information section S2; Sheppard *et al.*, 2013, 2016, 2019). We used a significance threshold of $P < 0.001$.

For both county- and district-level data, we assessed pairwise relationships between spatiotemporal variables using the spatial wavelet coherence technique. Spatial wavelet coherence tests for timescale-specific relationships between variables (Fig. S6). Specifically, the technique tests whether two spatiotemporal variables exhibit consistent phase differences and correlated magnitudes of oscillation through time and across space, as a function of timescale. Significance is determined by comparing spatial wavelet coherence values for real data with spatial wavelet coherences made from appropriately randomised, Fourier surrogate data sets (100 000 surrogate datasets) that retain the same temporal and spatial autocorrelation properties as the original time series but are otherwise

unrelated to each other (Supporting Information section S2; Theiler *et al.*, 1992; Schreiber and Schmitz, 2000; Sheppard *et al.*, 2013, 2016, 2017). We calculated how often observed spatial wavelet coherence between pairs of variables was ranked higher than coherences of surrogate data sets, aggregating across the timescale band of interest using an average rank-based method (Supporting Information section S2; Sheppard *et al.*, 2016). A P -value of less than 0.05 means that the average empirical spatial wavelet coherence rank was higher than the same quantity calculated for at least 95% of the surrogate data sets which represent the null hypothesis of no relationship. Ranks of actual spatial wavelet coherences in surrogate spatial wavelet coherences were also plotted against timescale. Finally, when two variables had significant spatial wavelet coherence over a timescale band, we calculated the mean phase difference between the variables over the band, $\bar{\theta}$, in units of π radians, to determine if oscillations had approximately in-phase ($|\bar{\theta}| = 0$ to 0.25), quarter-cycle ($|\bar{\theta}| = 0.25$ to 0.75) or anti-phase ($|\bar{\theta}| = 0.75$ to 1) relationships. We tested spatial wavelet coherence between deer abundance and weather and climate variables and hunter abundance, over the 3- to 7-year timescale band, where the majority of deer synchrony was present (see *Results*). We also used spatial wavelet coherence to test for relationships between deer abundance and DVCs, and between deer abundance and DVCs adjusted for traffic volume.

We calculated percentages of deer synchrony that could be explained by the synchrony of individual weather variables, through Moran effects, as well the percentage of DVC synchrony explained by deer synchrony, following the wavelet Moran theorem of Sheppard *et al.* (2016). As part of these procedures, we evaluated model “cross terms”, which are the component of synchrony that is due to variability explained by the drivers at a given location being synchronous with model residuals at other locations (Sheppard *et al.*, 2016). Cross terms must be small (<10%) in order for inferences about synchrony to be valid (Supporting Information section S2). There are reasons to expect large cross terms to be mitigated at larger spatial scales under some circumstance (Supporting Information section S2), one reason why we performed analyses at both county and district scales. The approach described here is most straightforwardly applied to predictors which are spatially as well as temporally resolved, for example, local weather variables as opposed to climate indices such as MEI. Attempts to use these techniques to quantify the fraction of deer synchrony explained by MEI were more complex, and were not needed for our research goals, so are in Supporting Information sections S2 (methods) and S3 (results).

To quantify the degree to which synchronising effects are responsible for cycling in statewide total deer and DVC time series, we adapted the standard Fourier surrogate procedure of Theiler *et al.* (1992). We constructed artificial time series data, for both variables for each location, that had the same spectral characteristics as the original data, except they were not spatially synchronised over the 3- to 7-year timescale band. We accomplished this by randomising phases of the Fourier transforms of the county-level time series (Supporting Information section S2). We summed each set of surrogate

time series spatially to produce surrogate statewide total time series for both deer and DVCs, representing the hypothetical case of no synchrony over 3- to 7-year timescales. We then compared these surrogate time series to the actual state-total deer abundance and DVC time series to determine to what extent additional variance and cycling intensity in the empirical state-total time series were attributable to synchrony.

Although wavelet tools were the most appropriate overall choice for our research goals and are now standard, some readers may be more familiar with Fourier analyses, which have a longer history. Also, there may be a perceived mismatch between our theory, which uses the Fourier language of stochastic processes, and our empirical analyses based on wavelets. In Supporting Information, after presenting supplementary wavelet results (Supporting Information section S3), we discuss why there is no real mismatch in approaches (beginning of Supporting Information section S4); but we also introduce (Supporting Information section S4) and apply (Supporting Information section S5) a comprehensive suite of alternative analyses of data, based solely on Fourier approaches. All main conclusions of our work were dually supported by both our wavelet and alternative Fourier approaches, increasing confidence in our results.

RESULTS

The wavelet mean field of county deer abundance time series revealed that synchrony occurred chiefly at 3- to 7-year timescales (Fig. 3a). The wavelet phasor mean field showed the strong statistical significance of this phenomenon (Fig. 3b). We therefore focused subsequent analysis on the 3- to 7-year timescale band. Mean field magnitude plots for all winter weather variables are in Fig. S7.

Spatial wavelet coherence demonstrated that deer abundance synchrony on 3- to 7-year timescales was partly caused by climatic Moran effects. Deer synchrony was related to winter snow depth (spatial wavelet coherence, $P = 0.05$, Table 1), in a near anti-phase relationship (mean phase difference

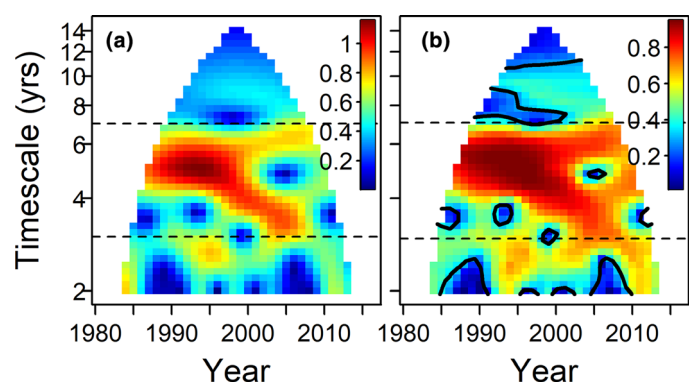


Figure 3 Wavelet mean field (a) and wavelet phasor mean field (b) magnitudes of deer abundance time series (*Methods*). Higher values in (a) and (b) indicate greater synchrony (a) or phase synchrony (b) at the indicated times and timescales. Contours on (b) indicate statistical significance of phase synchrony at $P = 0.001$. Horizontal lines in (a) and (b) indicate the timescales that were the focus of subsequent statistical analysis, 3–7 years.

between abundance and snow depth across 3- to 7-year timescales, in units of π radians, was $\bar{\theta} = 0.85$; Fig. S8d). Thus deer abundances tended to peak in years of below-average snow. No other local weather variables were significantly related with deer abundance (Table 1). Deer abundance was also related, with approximately quarter-cycle phase shifts, to the multivariate El Niño Southern Oscillation index ($P = 0.01$, $\bar{\theta} = -0.6$) and to the Pacific Decadal Oscillation ($P = 0.04$, $\bar{\theta} = -0.56$, Table 1, Fig. S8a and c), both averaged over the winter months (Dec_{*t-1*} to Mar_{*t*}, abbreviations MEI_w and PDO_w). These two indices were strongly coherent and in-phase with each other on 3- to 7-year timescales over 1981–2016 (wavelet coherence, $P = 0.0003$, $\bar{\theta} = 0.01$, Table S1). Deer abundance was also significantly coherent with growing-season MEI (Table 1), but likely only because MEI_w and growing-season MEI were coherent (Table S1). At 5-year periodicity, the quarter-cycle phase lags between deer abundance and MEI_w/PDO_w correspond to deer populations peaking about 1.4 or 1.5 years after mild winters. Significant spatial wavelet coherence with an environmental variable which is itself spatially synchronous (e.g., snow depth or some combination of weather variables related to MEI and PDO) is evidence of transmission of synchrony from the environment to deer via Moran effects (Supporting Information section S2; Sheppard *et al.*, 2016, 2019).

Snow depth and climate index results seemed to indicate distinct or partly distinct phenomena synchronising deer on different timescales within the 3- to 7-year band, and examining these distinct phenomena provide additional evidence that Moran effects on deer are occurring. Deer dynamics at 3- to 4-year timescales were not significantly spatially coherent with either MEI_w or PDO_w, which instead were strongly coherent with deer on 4- to 7-year timescales (Table 1, see also Fig. S9a and Table S2). In contrast, spatial wavelet coherence between snow depth and deer was not significant on 4- to 7-year timescales, but was significant on 3- to 4-year timescales (Table 1). Applying the wavelet Moran theorem, snow depth explained 16% of synchrony in deer abundance at 3- to 7-year timescales, but 40% of synchrony in deer abundance at 3- to 4-year timescales (Table 1; see also USDA district level results for the 3- to 4-year band, Table S2, which were similar but had smaller cross terms). The timescale bands 3 to 4 years and 4 to 7 years were chosen by examination of Fig. S9. The wavelet Moran theorem of Sheppard *et al.* (2016) could not straightforwardly be applied to estimate percentages of synchrony in deer explained by MEI_w, because MEI_w is not a spatially resolved variable (*Methods*). Such estimates are not necessary, however, for our argument that deer are environmentally synchronised in the 3- to 7-year band since this is already adequately demonstrated by our wavelet coherence results. See Supporting Information section S3 (also Fig. S10 and Table S3) for further discussion.

Deer synchrony on 3- to 7-year timescales was not caused by hunting. County-level hunter and deer abundances were not significantly spatially coherent ($P = 0.09$) over 3- to 7-year timescales (Table 1, Figs S9b, S11). Hunter abundance was significantly related to deer on shorter timescales, around 2 to 2.5-years ($P = 0.009$), and was in approximate anti-phase with deer abundance on those timescales ($\bar{\theta} = -0.84$; Table 1, Figs

Table 1 Summary of spatial wavelet coherence tests and related results using county-level data

Predictor	Response	Timescale	<i>P</i> -value	Mean phase ($\bar{\theta}$)	Synchrony explained	Average cross terms
Winter NAO	Abundance	3–7	0.4473			
Winter PDO	Abundance	3–7	0.0384	−0.5585		
Winter PDO	Abundance	3–4	0.2648			
Winter PDO	Abundance	4–7	0.0340	−0.6569		
Winter MEI	Abundance	3–7	0.0098	−0.5960		
Winter MEI	Abundance	3–4	0.1744			
Winter MEI	Abundance	4–7	0.0046	−0.6827		
Summer NAO	Abundance	3–7	0.3156			
Summer PDO	Abundance	3–7	0.1518			
Summer MEI	Abundance	3–7	0.0185	−0.8930		
Summer MEI	Abundance	3–4	0.2295			
Summer MEI	Abundance	4–7	0.0118	−0.9140		
Tmin	Abundance	3–7	0.5279			
Tmax	Abundance	3–7	0.4366			
Precipitation	Abundance	3–7	0.4562			
Snow Depth	Abundance	3–7	0.0530	0.8538	16.1854	9.0007
Snow Depth	Abundance	3–4	0.0101	0.8426	40.0303	9.6937
Snow Depth	Abundance	4–7	0.2232			
WSI	Abundance	3–7	0.2091			
Hunters	Abundance	3–7	0.0879			
Hunters	Abundance	2–2.5	0.0087	−0.8359	0.0581	−0.5092
Abundance	DVCs	3–7	0.0018	−0.0219	42.7297	33.2332
Abundance	Traffic-adj. DVCs	3–7	0.0000	−0.0245	40.6136	28.7796

P-values and mean phases are from tests of spatial wavelet coherence (*Methods*) of the variables in columns 1 and 2 over the indicated timescale band. Mean phases over the timescale band (units of π radians) are provided only when meaningful, that is, when spatial wavelet coherence was significant, $P < 0.05$, or marginally significant. A positive mean phase indicates the variable in the column *Response* is leading, and a negative mean phase indicates the variable in the column *Predictor* is leading. The *Synchrony explained* and *Average cross terms* columns, which give percentages, are based on the wavelet Moran theorem (*Methods*). When cross terms are low, synchrony explained is interpretable as the approximate percentage of synchrony in the response explainable as due to the synchrony in the predictor. Cross terms were low enough except for tests involving DVCs, for which USDA district-level results were more reliable (Table S2). *Synchrony explained* and *Average cross terms* are not reported for climate-index predictors because the climate indices are not spatially resolved (*Methods*). All values were rounded to display four digits. Abundance = deer abundance.

S8g, S9b). But these short-timescale results, while interesting (*Discussion*), are not particularly relevant for synchrony because deer showed limited synchrony on those timescales (Fig. 3).

The wavelet and wavelet phasor mean field magnitude plots for DVCs revealed time- and timescale-specific synchrony, and visual patterns were remarkably similar to those shown by deer (compare Figs 3a,b and Figs 4a,b). Spatial wavelet coherence showed that deer abundance and DVCs were significantly related ($P = 0.002$, Table 1) on 3- to 7-year timescales, and had a nearly in-phase relationship ($\bar{\theta} = -0.02$, Fig. S8e). Deer abundance explained 79% of the synchrony in DVCs when data were aggregated to USDA districts (Supporting Information section S3, Fig. S12 and Table S2). As a visual manifestation of this statistical result, a “predicted synchrony” plot, which shows patterns of synchrony in DVCs which would manifest if deer were the sole cause of DVC synchrony (see Supporting Information section S2 for how such a plot is produced), closely matched the patterns actually present in DVC synchrony (Fig. 4c). Statistical significance, phase relationships, and the amount of DVC synchrony explained by deer abundance remained similar after adjusting DVCs to account for fluctuations in traffic volume (Table 1, and Supporting Information section S3, Table S2, and Fig. S8f).

Statewide oscillations due to synchrony correspond to a typical difference of about 250 000 deer and about 2600 DVCs between peak and trough years (Fig. 5). Importantly, these high amplitude statewide oscillations in deer and DVCs disappear (Fig. 5) when synchrony between counties on 3- to 7-year timescales is removed via a randomisation procedure (*Methods*). Therefore, it is spatial synchrony that causes local dynamics to sum to a substantial semi-periodic oscillatory phenomenon on statewide spatial scales. Thus, the essence of our theoretical results was borne out in our empirical results (Fig. S13). Depending on assumptions made about DVC costs and reporting rates (Supporting Information section S2; Huijser et al., 2008; Marcoux and Riley, 2010; Conover, 2011), statewide DVC damages vary by US\$11–44Mn between peak and trough years.

Supplementary results using Fourier approaches (*Methods*, Supporting Information section S4) agreed with wavelet results, confirming the same main conclusions that: (1) synchrony in deer and DVCs was timescale specific and had a peak at 3- to 7-year timescales; (2) deer synchrony was due to environmental Moran effects and DVC synchrony was due to the synchronising effects of deer; and (3) statewide cycles in deer and DVCs occurred, and can be attributed to the time-scale-specific synchrony in these variables (Supporting Information section S5, Figs S14–S29, Table S4).

DISCUSSION

Overall, we demonstrated that timescale-specific Moran effects can cause cycles in a regional population. This is a new mechanism by which the environment can produce population cycles. Previous attempts to link environmental factors to population cycles have either been unsubstantiated (e.g. sun spots; Sinclair *et al.*, 1992; Selas *et al.*, 2004), or provided a useful but partial explanation for cycles, as in studies of tetraonids (Watson *et al.*, 2000) or small mammals (Kausrud *et al.*, 2008) which demonstrated that environmental factors tend to modify cycles produced by density-dependent factors, rather than producing them outright. Our study differs from previous work, in part because the new mechanism does not require a regular environmental oscillator like sun spots. Rather, it is sufficient for irregular environmental drivers such as winter climate to be coherent with populations over a particular timescale band, thereby inducing synchrony and leading to cycles in that band. We also presented what is, to our knowledge, the first demonstration that synchrony can be transmitted in a Moran-like effect from ecological to human systems (deer to DVCs). If climate change alters synchrony, as a growing number of papers indicate is likely occurring (Post and Forchhammer, 2004; Allstadt *et al.*, 2015; Defriez *et al.*, 2016; Koenig and Liebhold, 2016; Sheppard *et al.*, 2016; Shestakova *et al.*, 2016; Black *et al.*, 2018; Hansen *et al.*, 2020), our results show that cycles in populations and human systems may change as a consequence.

There are two alternative elaborations of our mechanism. First, environmental drivers may have produced small oscillations on 3- to 7-year timescales in county-level deer populations, and also brought these oscillations into synchrony, thereby causing them to sum across counties to produce state-wide cycles. Second, the local population oscillations may have been due partly to the intrinsic dynamics of deer, resulting from density-dependent effects, maternal effects, or other mechanisms of nonlinear dynamics. Synchronous environmental drivers would then have brought the intrinsically oscillating local dynamics into synchrony. The difference between these alternatives is whether local population oscillations were produced and synchronised, or synchronised but not produced, by environmental drivers. The alternatives would be

difficult to distinguish, but the former mechanism may be more likely because winter climate is known to influence ungulate dynamics (Post and Forchhammer, 2004; Grøtan *et al.*, 2005; Mysterud *et al.*, 2008; Hegel *et al.*, 2012), and we are unaware of any evidence suggesting that deer populations are intrinsically cyclic. In either case our mechanism is the same whereby Moran effects synchronise local dynamics in a timescale-specific manner, and then local dynamics sum to produce cycles. Randomisations that removed synchrony but preserved local fluctuations eliminated the state-wide cycles (Fig. 5), demonstrating that synchrony likely produced them.

Large-scale climatic patterns and local winter weather are known to influence synchrony via Moran effects in other ungulates, including reindeer, caribou (Post and Forchhammer, 2002, 2004; Aanes *et al.*, 2003; Hegel *et al.*, 2012), roe deer (Grøtan *et al.*, 2005) and musk oxen (Post and Forchhammer, 2002), and thus the cycling mechanism we observed may also occur in other ungulates. Here winter snow depth and MEI_w/PDO_w were the primary determinants of deer synchrony. Deer populations lagged MEI_w by 1–2 years, a similar delay to other reported lag times of climatic effects on deer populations (Forchhammer *et al.*, 1998; Post and Stenseth, 1998). Winter weather and climate probably influenced deer because deeper snow limits access to winter food, which then increases susceptibility to starvation or predators and reduces parturition rates (Myserud *et al.*, 2008; Hegel *et al.*, 2012). Winter weather influences deer beyond WI, so timescale-specific synchrony may extend further than WI. Cycling over larger regions may then be even stronger than what we documented because a larger number of synchronised local populations can accentuate the effect we described.

Hunters were not the principal driver of deer synchrony. These results are consistent with the hypothesis that hunters can regulate deer populations over short timescales and small areas (Fryxell *et al.*, 1991; DeNicola and Williams, 2008) but have limited effects over longer timescales and larger areas (Brown *et al.*, 2000; Simard *et al.*, 2013). The lack of longer timescale (3- to 7-year) spatial wavelet coherence between hunters and deer abundance likely also relates to the facts that hunters typically prefer to shoot bucks, the removal of which has limited population effects; and the state regulates antlerless harvest to maintain desirable population sizes.

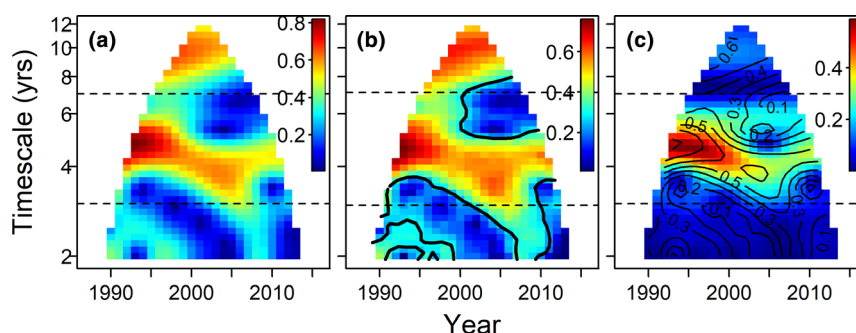


Figure 4 Wavelet mean field (a) and wavelet phasor mean field (b) magnitudes and predicted synchrony (c) of DVCs. Colors, contours and horizontal lines in (a) and (b) indicate the same as in Fig. 3a and b, but for DVC data. Colors in (c) show synchrony in DVCs predicted by a wavelet model with sole predictor deer abundance, while contours in (c) show the actual wavelet mean field magnitude of DVCs from (a), for comparison. Agreement is good, giving a visual indication of the statistical result that deer synchrony explains DVC synchrony.

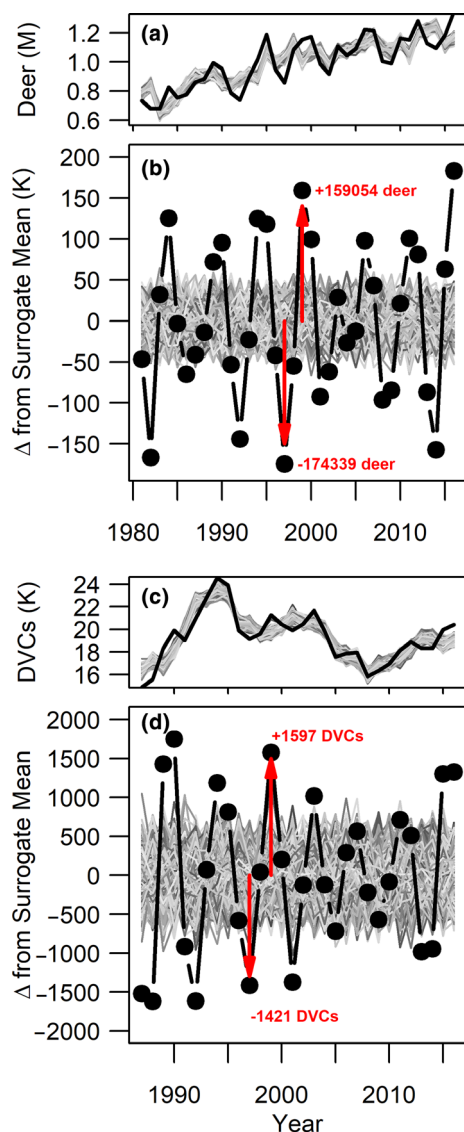


Figure 5 Magnitude of the effects of synchrony on state-total deer abundance and DVC fluctuations. Small panels show state-total deer abundance ((a), in millions) and DVC ((c), in thousands) time series (black lines) and surrogate totals obtained via a randomisation procedure (*Methods*) that eliminates synchrony among counties at 3- to 7-year timescales (grey lines, 1000 surrogates plotted). Increased variation and semi-periodic oscillations due to synchrony are particularly notable when trends and long-timescale (longer than 7 years) variability are filtered out by subtracting the mean of the grey lines ((b) for deer, in thousands; (d) for DVCs). Δ represents the difference in values from the surrogate mean. Red arrows highlight examples of the strong cycling that is attributable to synchrony.

Our results provide a previously unrecognised applied motivation for studies of synchrony in populations. Fluctuations of a quarter million deer, statewide, caused by synchrony, likely will have considerable consequences for agricultural crop damage, forest regeneration (Côté *et al.* 2004), and hunting success, all of which can have socioeconomic impacts. We also showed that Moran effects subsequently pass from deer to DVCs in a cascading manner. Deer synchrony almost certainly caused DVC synchrony rather than the opposite

causation, because DVCs were too infrequent to meaningfully drive deer fluctuations (Fig. 2), and if they did an anti-phase relationship would have been found (as opposed to the in-phase relationship we observed). Thus Moran effects are ultimately responsible for synchrony of DVCs, and synchrony causes fluctuations of more than 2500 annual documented DVCs through time. Such fluctuations may influence insurance and accident recovery industries, though we have not inquired whether a fluctuation of this magnitude is big enough to be of substantial concern to these industries. Our results provide another reason that additional studies of climate-change influences on synchrony (Hansen *et al.*, 2020) should be undertaken: such influences may alter the cycling of populations, including populations of socioeconomic importance.

An important aspect of the phenomena we explore is their specificity to certain timescales. Deer cycles would not have manifested had deer synchrony not been specific to certain timescales. Timescale specificity in synchrony is now known to be common (Sheppard *et al.*, 2016, 2017, 2019; Walter *et al.*, 2017; Anderson *et al.*, 2019; Haynes *et al.*, 2019). Many past analyses of synchrony have used correlation methods (Liebhold *et al.*, 2004) that conflate timescales, but this can hinder detection of synchronous phenomena and inferences of drivers of synchrony by obscuring synchrony on some timescales with asynchronous dynamics on other timescales (Sheppard *et al.*, 2016). The methods used here (Sheppard *et al.*, 2016, 2017, 2019; Walter *et al.*, 2017) were able to isolate the timescales on which synchrony occurred, facilitating precise determination of drivers of synchrony. Historically, determination of causes of synchrony was called difficult (Kendall *et al.*, 2000; Liebhold *et al.*, 2004; Abbott, 2007), but in our previous work (Sheppard *et al.*, 2016, 2017, 2019; Walter *et al.*, 2017), and again here, we showed that using timescale-specific methods can help ameliorate this difficulty and can reveal new phenomena and mechanisms.

ACKNOWLEDGEMENTS

D. Lyden, J. Steinglein and the WIDNR for data; D. Storm, T. Van Deelen, J. Millsbaugh, J. Fox, K. Haynes and A. Liebhold for consultation; and anonymous referees for very useful feedback and some code. Funding was provided by the James S McDonnell Foundation, United States National Science Foundation grants 1442595, 1714195 and 2023474, United States Department of Agriculture award 2016-67012-24694 and The Nature Conservancy.

Author Contributions: TLA and DCR conceived the project; RER provided assistance with data curation; TLA, DCR and LWS analysed the data; TLA and DCR wrote manuscript; all authors provided extensive editing and feedback on the analysis and manuscript.

DATA AVAILABILITY STATEMENT

All data are available from the Dryad digital repository: <https://doi.org/10.5061/dryad.rn8pk0p85>. All data and code producing this paper are also archived at www.github.com/reumandc/TomAnderson_WIdeer. Analyses leading to the paper can be re-run and the paper re-compiled via the codes there.

REFERENCES

- Aanes, R., Sæther, B.-E., Solberg, E.J., Aanes, S., Strand, O. & Øritsland, N.A. (2003). Synchrony in Svalbard reindeer population dynamics. *Can. J. Zool.*, 81, 103–110.
- Abbott, K.C. (2007). Does the pattern of population synchrony through space reveal if the Moran effect is acting? *Oikos*, 116, 903–912.
- Addison, P.S. (2002). *The Illustrated Wavelet Transform Handbook: Introductory Theory and Applications in Science, Engineering, Medicine and Finance*, 1st edn. Institute of Physics Publishing, Bristol.
- Allstadt, A.J., Liebhold, A.M., Johnson, D.M., Davis, R.E. & Haynes, K.J. (2015). Temporal variation in the synchrony of weather and its consequences for spatiotemporal population dynamics. *Ecology*, 96, 2935–2946.
- Anderson, T., Sheppard, L., Walter, J., Hendricks, S., Levine, T., White, D. *et al.* (2019). The dependence of synchrony on timescale and geography in freshwater plankton. *Limnol. Oceanogr.*, 64, 483–502.
- Bjørnstad, O.N. (2000). Cycles and synchrony: Two historical “experiments” and one experience. *J. Anim. Ecol.*, 69, 869–873.
- Black, B., van der Sleen, P., Di Lorenzo, E., Griffin, D., Sydeman, W., Dunham, J. *et al.* (2018). Rising synchrony controls western North American ecosystems. *Glob. Change Biol.*, 24, 2305–2314.
- Brown, T.L., Decker, D.J., Riley, S.J., Enck, J.W., Lauber, T.B., Curtis, P.D. *et al.* (2000). The future of hunting as a mechanism to control white-tailed deer populations. *Wildl. Soc. Bull. (1973-2006)*, 28(4), 797–807.
- Buonaccorsi, J.P., Elkinton, J.S., Evans, S.R. & Liebhold, A.M. (2001). Measuring and testing for spatial synchrony. *Ecology*, 82, 1668–1679.
- Ciuti, S., Jensen, W.F., Nielsen, S.E. & Boyce, M.S. (2015). Predicting mule deer recruitment from climate oscillations for harvest management on the northern great plains. *J. Wildl. Manag.*, 79, 1226–1238.
- Conover, M.R. (2011). Impacts of deer on society. In *Biology and Management Of White-Tailed Deer* (ed Hewitt, D.G.). Book Section. CRC Press, Boca Raton, FL, pp. 399–408.
- Côté, S.D., Rooney, T.P., Tremblay, J.-P., Dussault, C. & Waller, D.M. (2004). Ecological impacts of deer overabundance. *Annu. Rev. Ecol. Syst.*, 35, 113–147.
- Defriez, E.J. & Reuman, D.C. (2017a). A global geography of synchrony for marine phytoplankton. *Glob. Ecol. Biogeogr.*, 26, 867–877.
- Defriez, E.J. & Reuman, D.C. (2017b). A global geography of synchrony for terrestrial vegetation. *Glob. Ecol. Biogeogr.*, 26, 878–888.
- Defriez, E.J., Sheppard, L.W., Reid, P.C. & Reuman, D.C. (2016). Climate change related regime shifts have altered spatial synchrony of plankton dynamics in the North Sea. *Glob. Change Biol.*, 22, 2069–2080.
- DeNicola, A.J. & Williams, S.C. (2008). Sharpshooting suburban white-tailed deer reduces deer-vehicle collisions. *Human-Wildlife Interactions*, 2, 28–33.
- Forchhammer, M.C., Stenseth, N.C., Post, E. & Landvatn, R. (1998). Population dynamics of Norwegian red deer: Density-dependence and climatic variation. *Proc. R. Soc. Lond. B Biol. Sci.*, 265, 341–350.
- Fryxell, J.M., David, J.T.H., Lambert, A.B. & Smith, P.C. (1991). Time lags and population fluctuations in white-tailed deer. *J. Wildl. Manag.*, 55, 377–385.
- Grøtan, V., Saether, B.-E., Engen, S., Solberg, E.J., Linnell, J.D., Andersen, R. *et al.* (2005). Climate causes large-scale spatial synchrony in population fluctuations of a temperate herbivore. *Ecology*, 86, 1472–1482.
- Hansen, B.B., Grøtan, V., Herfindal, I. & Lee, A.M. (2020). The Moran effect revisited: Spatial population synchrony under global warming. *Ecography*, 43, 1–12.
- Haynes, K.J., Walter, J.A. & Liebhold, A.M. (2019). Population spatial synchrony enhanced by periodicity and low detuning with environmental forcing. *Proc. R. Soc. B*, 286, 20182828.
- Hegel, T.M., Verbyla, D., Huettmann, F. & Barboza, P.S. (2012). Spatial synchrony of recruitment in mountain-dwelling woodland caribou. *Popul. Ecol.*, 54, 19–30.
- Hopson, J. & Fox, J.W. (2019). Occasional long distance dispersal increases spatial synchrony of population cycles. *J. Anim. Ecol.*, 88, 154–163.
- Huijser, M.P., McGowen, P.T., Clevenger, A.P. & Ament, R. (2008). *Wildlife-vehicle collision reduction study: Best practices manual*. Report to Congress. U.S. Department of Transportation, Federal Highway Administration, Washington, D.C., USA.
- Kausrud, K.L., Mysterud, A., Steen, H., Vik, J.O., Østbye, E., Cazelles, B. *et al.* (2008). Linking climate change to lemming cycles. *Nature*, 456, 93–97.
- Kendall, B.E., Bjørnstad, O.N., Bascompte, J., Keitt, T.H. & Fagan, W.F. (2000). Dispersal, environmental correlation, and spatial synchrony in population dynamics. *Am. Nat.*, 155, 628–636.
- Koenig, W.D. & Liebhold, A.M. (2016). Temporally increasing spatial synchrony of North American temperature and bird populations. *Nat. Clim. Chang.*, 6, 614–617.
- Krebs, C. (2013). *Population fluctuations in rodents*. University of Chicago Press, Chicago.
- Krebs, C., Boonstra, R. & Boutin, S. (2018). Using experimentation to understand the 10-year snowshoe hare cycle in the boreal forest of North America. *J. Anim. Ecol.*, 87, 87–100.
- Liebhold, A., Koenig, W.D. & Bjørnstad, O.N. (2004). Spatial synchrony in population dynamics. *Annu. Rev. Ecol. Syst.*, 35, 467–490.
- Marcoux, A. & Riley, S.J. (2010). Driver knowledge, beliefs, and attitudes about deer-vehicle collisions in southern Michigan. *Human-Wildlife Interactions*, 4, 47–55.
- Martínez-Padilla, J., Redpath, S., Zeineddine, M. & Mougeot, F. (2014). Insights into population ecology from long-term studies of red grouse *Lagopus lagopus scotius*. *J. Anim. Ecol.*, 83, 85–98.
- Myers, J. & Cory, J. (2013). Population cycles in forest Lepidoptera revisited. *Annu. Rev. Ecol. Syst.*, 44, 565–592.
- Myers, J.H. (2018). Population cycles: Generalities, exceptions and remaining mysteries. *Proc. R. Soc. B*, 285, 20172841.
- Mysterud, A., Yoccoz, N.G., Langvatn, R., Pettorelli, N. & Stenseth, N.C. (2008). Hierarchical path analysis of deer responses to direct and indirect effects of climate in northern forest. *Philos. Trans. R. Soc. Lond., B*, 363, 2357–2366.
- Nilssen, A., Tenow, O. & Bylund, H. (2007). Waves and synchrony in *Epirrita autumnata/Operophtera brumata* outbreaks II: Sunspot activity cannot explain cyclic outbreaks. *J. Anim. Ecol.*, 76, 269–275.
- Post, E. & Forchhammer, M.C. (2002). Synchronization of animal population dynamics by large-scale climate. *Nature*, 420, 168–171.
- Post, E. & Forchhammer, M.C. (2004). Spatial synchrony of local populations has increased in association with the recent Northern Hemisphere climate trend. *Proc. Natl. Acad. Sci. USA*, 101, 9286–9290.
- Post, E. & Stenseth, N.C. (1998). Large-scale climatic fluctuation and population dynamics of moose and white-tailed deer. *J. Anim. Ecol.*, 67, 537–543.
- Reuman, D.C., Anderson, T.L., Walter, J.A., Zhao, L. & Sheppard, L.W. (2019). R package wsyn: wavelet approaches to studies of synchrony in ecology and other fields. Comprehensive R Archive Network. <https://CRAN.R-project.org/package=wsyn>.
- Rodionov, S. & Assel, R.A. (2003). Winter severity in the Great Lakes region: A tale of two oscillations. *Clim. Res.*, 24, 19–31.
- Rohani, P., Earn, D.J. & Grenfell, B.T. (1999). Opposite patterns of synchrony in sympatric disease metapopulations. *Science*, 286, 968–971.
- Schreiber, T. & Schmitz, A. (2000). Surrogate time series. *Physica D*, 142, 346–382.
- Selas, V., Hogstad, O., Kobro, S. & Trond, R. (2004). Can sunspot activity and ultraviolet-b radiation explain cyclic outbreaks of forest moth pest species? *Proc. R. Soc. B*, 27, 1897–1901.
- Sheppard, L., Hale, A., Petkoski, S., McClintock, P. & Stefanovska, A. (2013). Characterizing an ensemble of interacting oscillators: The mean-field variability index. *Phys. Rev. E*, 87, 012905.
- Sheppard, L.W., Bell, J.R., Harrington, R. & Reuman, D.C. (2016). Changes in large scale climate alter spatial synchrony of aphid pests. *Nat. Clim. Chang.*, 6, 610–613.

- Sheppard, L.W., Defriez, E.J., Reid, P.C. & Reuman, D.C. (2019). Synchrony is more than its top-down and climatic parts: Interacting Moran effects on phytoplankton in British seas. *PLoS Comput. Biol.*, 15, e1006744.
- Sheppard, L.W., Reid, P.C. & Reuman, D.C. (2017). Rapid surrogate testing of wavelet coherences. *EPJ Nonlinear and Biomedical Physics*, 5, 1–5.
- Shestakova, T.A., Gutiérrez, E., Kirilyanov, A.V., Camarero, J.J., Génova, M., Knorre, A.A. *et al.* (2016). Forests synchronize their growth in contrasting Eurasian regions in response to climate warming. *Proc. Natl. Acad. Sci. USA*, 113, 662–667.
- Simard, M.A., Dussault, C., Huot, J. & Côté, S.D. (2013). Is hunting an effective tool to control overabundant deer? A test using an experimental approach. *J. Wildl. Manag.*, 77, 254–269.
- Sinclair, A., Gosline, J., Holdsworth, G., Krebs, C., Boutin, S., Smith, J. *et al.* (1992). Can the solar cycle and climate synchronize the snowshoe hare cycle in Canada? Evidence from tree rings and ice cores. *Am. Nat.*, 141, 173–198.
- Stenseth, N.C., Chan, K.-S., Tong, H., Boonstra, R., Boutin, S., Krebs, C.J. *et al.* (1999). Common dynamic structure of Canada lynx populations within three climatic regions. *Science*, 285, 1071–1073.
- Stenseth, N.C., Ehrlich, D., Rueness, E.K., Lingjaerde, O.C., Chan, K.S., Boutin, S. *et al.* (2004). The effect of climatic forcing on population synchrony and genetic structuring of the Canadian lynx. *Proc. Natl. Acad. Sci. USA*, 101, 6056–6061.
- Theiler, J., Eubank, S., Longtin, A., Galdrikian, B. & Farmer, J.D. (1992). Testing for nonlinearity in time series: The method of surrogate data. *Physica D*, 58, 77–94.
- U.S. Department of the Interior, U.S. Fish & Wildlife Service, U.S. Department of Commerce & U.S. Census Bureau. (2011). National survey of fishing, hunting, and wildlife-associated recreation.
- Vasseur, D.A. & Fox, J.W. (2009). Phase-locking and environmental fluctuations generate synchrony in a predator-prey community. *Nature*, 460, 1007–1010.
- Walter, J.A., Sheppard, L.W., Anderson, T.L., Kastens, J.H., Bjørnstad, O. N., Liebhold, A.M. *et al.* (2017). The geography of spatial synchrony. *Ecol. Lett.*, 20, 801–814.
- Watson, A., Moss, R. & Rothery, P. (2000). Weather and synchrony in 10-year population cycles of rock ptarmigan and red grouse in Scotland. *Ecology*, 81, 2126–2136.
- Wisconsin Department of Natural Resources. (2001). Management workbook for white-tailed deer.

SUPPORTING INFORMATION

Additional supporting information may be found online in the Supporting Information section at the end of the article.

Editor, Bernd Blasius

Manuscript received 16 January 2020

First decision made 30 September 2020

Manuscript accepted 29 October 2020